The Color of Halftone Tints

J. A. Stephen Viggiano*

ABSTRACT

The relationship between density, reflectance, and color is used to derive a formula for calculating the color of a halftone tint. This involves applying the Yule-Neilsen Equation at each point in the spectrum.

The details of an experiment providing perliminary verification of this approach are presented. Details of additional work in progress are also discussed.

INTRODUCTION

The Yule-Neilsen Model[1] has been successfully used to predict the density of black-and-white halftone tints, given the solid ink density and the halftone dot area on the paper. While the halftone dot area on the paper (a_p) is not convienently measured directly, it may be calculated from the routinely measured dot area on film (a_f) once the dot gain function has been determined.[2]

Because "color" has often been measured in the graphic arts by recording the Red, Green, and Blue components of density (despite urgings to the contrary),[3] it seems tempting to apply the Yule-Neilsen model for each of these channels in much the same way as is done for black-and-white. This would permit the prediction of the Red, Green, and Blue density components, given a_p and the corresponding density components of the solid.

However, this approach has never really become popular. Some investigators have noted significant errors, particularly when attempting to predict the color of multi-color overprinting tints and with colorimetric (which is characteristically wide-band) measurement. In fact, Pobboravsky resorted to a second-degree polynomial, which provided better fit than Yule-Neilsen theory.[4]

*Graduate Student, Rochester Institute of Technology, School of Printing.

It has been suggested by the author that the color of a halftone tint may be accurately predicted by applying the Yule-Neilsen model at each wavelength of the spectrum, rather than just for three rather wide bands.[5] The result would be a prediction of the spectrum of the tint, which could then be integrated to obtain predictions of (X, Y, Z) or CIELUV color coordinates. Similarly, for quality control applications, the Status "T" (wideband) or SPI (narrowband) densitometer responses could be predicted.

The Yule-Neilsen Model- The Yule-Neilsen model provides an intimate link between dot area on paper and the density of a halftone tint (D_t), given the density of the solid print (D_s), and the value of a parameter, n. (Usually, a value in the region of 1.7 is recommended.)[6] Specifically,

$$D_t = -n \log[1 - a_p(1 - 10^{-D_s/n})] \quad (1)$$

(The symbol "u" is sometimes substituted for the "1/n"; this is a subtle pun on the fact that u is the inverse of n.)

Substituting reflectances for densities we obtain:

$$R_t = [1 - a_p(1 - R_s^u)]^n \quad (2)$$

We may invert (1) and (2) to obtain the dot area as a function of the densities (or reflectances):

$$a_p = \frac{1 - 10^{-D_t/n}}{1 - 10^{-D_s/n}} = \frac{1 - R_t^u}{1 - R_s^u} \quad (3)$$

These equations have been verified for black dots on white paper. Black inks have characteristically flat spectral reflectance curves (throughout the visible spectrum), so the Yule-Neilsen model seems to work reasonably well with inks having constant reflectance in the band being measured.

Colored inks, by definition, do not have constant reflectances throughout the visible spectrum (i.e., they are selective), and, by nature, do not exhibit sharp changes in reflectance between densitometer bands. Rather, the reflectance of an ink will vary throughout the entire spectrum, from both band to band and within each band. It will be demonstrated how this variation causes problems with wide-band measurements.

The Inverse Schwartz Inequality- If we consider two positive numbers, a and b, the square root of their sum will be less than the sum of their square roots. Symbolically:

$$\sqrt{a} + \sqrt{b} > \sqrt{a + b} \quad (4)$$

By way of example, if a = 16 and b = 9, $\sqrt{a} + \sqrt{b} = 7$, but $\sqrt{a+b} = 5$.

As a matter of fact, inequalities of this type may be constructed for any root greater than one. Of particular interest is the 1.7-th root, which yields 8.7505 for the sum of the roots, but 6.6423 for the root of the sum. If we correct the latter for the sum, we observe a difference of about 1 percent. Larger errors result when the two numbers are more dissimilar in relative magnitude. The reflectance of an ink film, for example, may vary by a factor of 10 within the bandwidth of a Status "T" densitometer. (See Figures 1, 2, and 3 for spectral density curves of process colors - for solids and tints.)

The Integration of Densities- With wideband instrumentation, such as Status "T" densitometers, the individual reflectances for each wavelength are added together (integrated) to yield the reflectance over that particular band. This is the mechanism of light; different wavelengths are reflected and received in parallel, so the instrument does not need to actively integrate across the spectrum. Nonetheless, the individual reflectances may be considered separately.

In practice, the reflectance of each wavelength will be weighted by the spectral product of that particular channel of the instrument, so the spectral characteristics of the source, filter, photodetector, etc. are taken into consideration.

Without going far afield, we can see that if the reflectances are added together before the n-th root is taken (i.e., before they are raised to the u-th power), we are in danger of violating the Inverse Schwartz Inequality, and thereby taint our results with a bias term, yielding error.

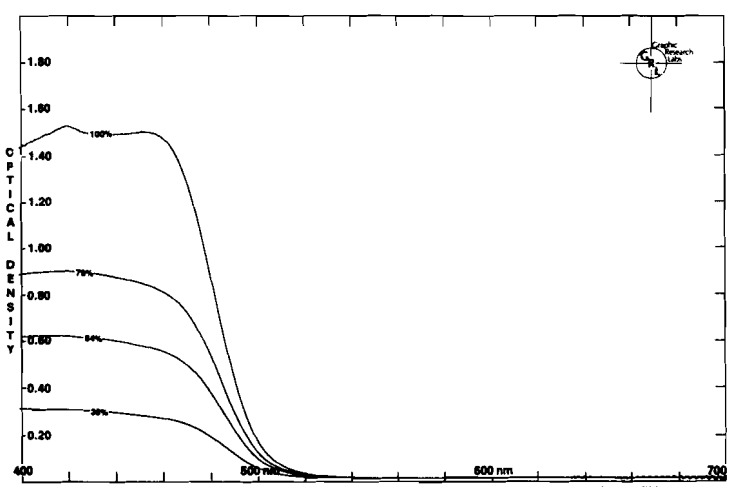

Figure 1.
Spectral Density of a Yellow Overlay

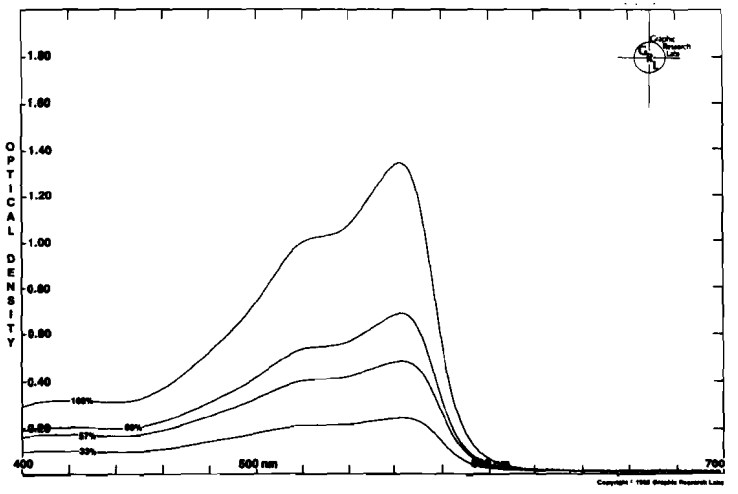

Figure 2.

Spectral Density of a Magenta Overlay

THE SPECTRAL YULE-NEILSEN MODEL

The author has suggested that the Yule-Neilsen model be applied not for three wide bands, but rather at each wavelength in the visible spectrum.[5] Because light of only a single wavelength is considered at a time, there is no need to sum (integrate) the reflectances before they are raised to the u-th power. In this way the Inverse Schwartz Inequality is avoided, and greater precision should be possible.

Once the reflectances of the tint at each wavelength are predicted (by repeated application of Eq. (2)), they may be summed according to the three weighting functions $kS(\lambda)\bar{x}(\lambda)$, $kS(\lambda)\bar{y}(\lambda)$, and $kS(\lambda)\bar{z}(\lambda)$ to obtain the CIE Tristimulus Values X, Y, and Z. λ is the wavelength under consideration; $S(\lambda)$ is the relative spectral power distribution of the illuminant; $\bar{x}(\lambda)$, $\bar{y}(\lambda)$, and $\bar{z}(\lambda)$ are the color matching functions; and k is a constant which normalizes the sum of $kS(\lambda)\bar{y}(\lambda)$ to 100. It is recommended that the CIE 1931 color matching functions be used.[7]

These tristimulus values should be transformed into one of the uniform color spaces if they are to be compared. Of the two CIE standard uniform color spaces, the author would recommend CIELUV, because calculations of saturation are important in subtractive processes, such as printing. (Recall that saturation is one of the two coordinates plotted on the GATF Color Hexagon.[8]) Saturation values do not seem to be tractable in the other CIE uniform color space, CIELAB.[9]

Calculation of the L*, u*, v* coordinates (and, possibly, the saturation, chroma, etc.) of the tint from the predicted spectral reflectance function completes the process of computing the tint's color.

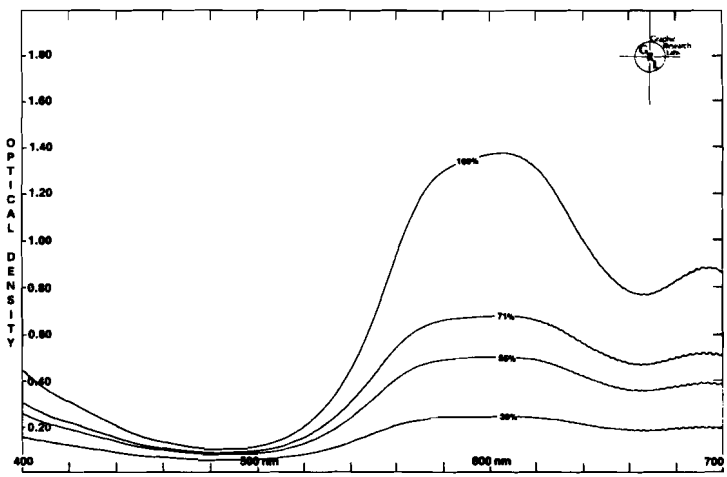

Figure 3.
Spectral Density of a Cyan Overlay.

EXPERIMENTAL APPROACH

An experiment was conducted to test the validity of this approach. Essentially, the approach was to generate a series of tints and solids in several colors, photometrically measure the dot areas of the tints, measure the spectral densities of the tints and solids at 16 wavelengths, and compare the spectral tint densities as measured with the spectral tint densities as predicted by the Spectral Yule-Neilsen model. The square root of the average of the squares of these deviations is the Root Mean Square (RMS) Error, or Standard Deviation (SD). If this value is significantly greater than the amount of error we would expect to be caused by the measuring equipment alone, we must conclude that there is a significant amount of bias inherent in the model.

The CIELUV coordinates will also be calculated, and color difference values will be computed to provide an additional check of fit.

Further, for illustrative purposes, the spectral densities will be converted into reflectances, summed according to the weighting functions to yield the tristimulus values X, Y, and Z. The Yule-Neilsen model will be applied to each tristimulus value separately, so that the tint color may be predicted by

wideband theory. The color difference between predicted and observed will be computed for each tint, using both wideband and spectral theory. It is expected that the color errors from the wideband calculations will be higher than for the spectral calculations.

The Overlay Approach- Daniels and Pearson[6] have suggested that halftone tints on overlay proofing material (e.g., Color Key®), when placed on a printing substrate, may be used to simulate halftone tints produced on a press. Indeed, this is the aim of these materials. Because the actual dots are on a transparent non-scattering substrate, the area of the dots may be read photometrically by transmission, a straightfoward technique.

The overlay is placed base side up on a piece of paper (or other printing substrate) to simulate press-printed dots on that paper. Quite naturally a problem with this approach is that it permits only a simulation of press-printed dots on paper. There are a number of important differences between the overlay film and press printed dots. The most obvious of these is caused by the plastic support film; halftone dots do not normally have a covering of glossy plastic. They may, however, have a varnish overcoat, which is similar.

Nonetheless, hypothetical varnish overcoats notwithstanding, steps should be taken to minimize the effects (particularly the gloss effects) of this sheet on the spectral density readings. If the measuring instrument has an integrating sphere, the specular component should be excluded.

Significance of Errors- Most densitometers (including spectral densitometers) are designed to exhibit a maximum deviation of 0.02 density units from standard. This seems to be a reasonable tolerance. If a flat distribution of errors is assumed, we would expect a standard deviation, then, of 0.0115 to be caused by measurement error alone. However, the standard deviation (RMS Error) actually observed will differ from this value because of chance variation.

A table of Chi-Square may be consulted to obtain a factor by which this "target" standard deviation may be multiplied to obtain a critical value. For two targets in each of the three process colors, three tint blocks per target, and 16 points throughout the spectrum, 288 differences will be calculated. For 288 degrees of freedom and at the 5 percent significance level, the factor is 1.07. (Actually, a formula was used because most tables do not go as high as 288 degrees of freedom.)

This comparison is possible when testing for lack of fit with the spectral Yule-Neilsen model. It is not, however, valid for comparing one color error (observed - predicted) with another for the same object (but different theories). This is because of the naturally high correlation between color coordinates of the same object predicted by two different theories. As was mentioned before, the color errors will be calculated for illustrative purposes only.

EXPERIMENTAL METHODOLOGY

The Test Target- Halftone tint screens were stripped into a frisket mask to produce a small test target, containing dot areas of approximitely 30, 50, and 70 percent halftone dot area. An open block was left for producing a solid, and a solid area was ruled out to produce a clear area on the overlay film (which serves as the reference). The size of each of these blocks was approximitely 35 mm square, and the screen ruling was approximitely 52 lines per cm (133 lines per inch). The dots were eliptical, and oriented 45 degrees from the horizontal axis; a standard dot orientation.

Colors- The process colors, Cyan, Magenta, and Yellow, were selected for the verification of the spectral Yule-Neilsen model. Not only are color proofing films readilly available in these colors, but these are the colors most printers would be interested in (yielding a more viable inference space). In addition, these colors provide a relatively "balanced" representation of all colors.

Materials- 3-M Color Key material was supplied by Mr. George Leyda of 3-M. After determination of the dot areas, the films were overlaid (base side up) on 100 gram/meter^2 Mead Print-Flex coated paper.

Instrumentation- A Tobias PCT Dot Area Meter, loaned by Mr. Philip Tobias, was used to measure the dot areas of the proofing films. The readings were made through complementary filters (e.g., blue filter for the yellow overlay) to increase the transmission contrast of the film, which is characteristically low. The device was zeroed out on the clear block for each overlay, and normalized to 100 percent on the solid blocks. This also was necessitated by the relatively low transmission contrast of the films.

The Shimadzu UV-210 Spectrophotometer/Spectrodensitometer in the RIT Ink and Color Laboratory was used to measure the spectral densities of the target patches. White paper, overlaid with clear proofing film, served as the reference white. Care was taken so that the reference white was selected from the same target as the other patches. This is equivalent to the standard graphic arts practice of zeroing (or nulling) a densitometer on the sheet.

Because the illumination in the Shimadzu is precisely normal to the sample and reference, the specular component is excluded. This serves to minimize the effects of gloss on measurements taken on integrating-sphere type spectrophotometers.

A slit width of 2 nm was chosen, and digital readings were generated every 20 nm between 400 and 700 nm. (This sequence may be abbreviated as 400 [20] 700 nm.) These sampling points are fairly standard for abridged spectrophotometery. Continuous curves were also generated throughout this region. Samples of these curves were presented in Figures 1, 2, and 3.

EXPERIMENTAL RESULTS

Spectrophotometric Data- The spectral densities of each of the 18 tint blocks and six solids are presented in Table 1, grouped by the target from which they were cut. The reference white in all cases was a piece of clear overlay film from the same target as the patches being measured, placed on a piece of the same paper as was used for the sample patches.

Table 1 also contains the halftone dot areas as measured by transmission by the PCT dot area meter.

	Target #1 (Yellow)					Target #2 (Yellow)			
nm	Dt 30	Dt 50	Dt 70	Ds	nm	Dt 30	Dt 50	Dt 70	Ds
400	0.241	0.543	0.810	1.447	400	0.314	0.626	0.877	1.425
420	0.236	0.553	0.831	1.549	420	0.310	0.629	0.893	1.535
440	0.230	0.542	0.815	1.509	440	0.295	0.606	0.867	1.498
460	0.220	0.507	0.773	1.509	460	0.270	0.560	0.809	1.491
480	0.171	0.370	0.549	0.935	480	0.195	0.395	0.551	0.933
500	0.058	0.095	0.129	0.187	500	0.060	0.106	0.130	0.188
520	0.016	0.017	0.025	0.036	520	0.018	0.024	0.018	0.033
540	0.009	0.005	0.010	0.014	540	0.011	0.012	0.004	0.014
560	0.008	0.003	0.004	0.012	560	0.009	0.010	0.004	0.010
580	0.007	0.001	0.003	0.010	580	0.008	0.007	0.004	0.009
600	0.006	0.002	0.005	0.010	600	0.007	0.005	0.004	0.009
620	0.010	0.008	0.009	0.013	620	0.008	0.005	0.004	0.007
640	0.008	0.001	0.000	0.011	640	0.009	0.005	0.004	0.008
660	0.009	0.001	0.003	0.009	660	0.008	0.004	0.004	0.005
680	0.012	0.013	0.013	0.013	680	0.005	0.004	0.004	0.010
700	0.010	0.008	0.010	0.010	700	0.005	0.004	0.004	0.009
a_p	0.31	0.59	0.76		a_p	0.38	0.64	0.79	

Legend: nm is the wavelength in nanometers;
a_p is the halftone dot area on the paper;
Dt 30, Dt 50, and Dt 70 are the spectral densities of the (nominally) 30%, 50%, and 70% tint blocks; and
Ds is the spectral density of the solid.

TABLE 1.

Dot Areas and Observed Spectral Densities.

Table 1 (Continued).

Target #3 (Magenta)

nm	Dt 30	Dt 50	Dt 70	Ds
400	0.080	0.137	0.179	0.215
420	0.082	0.146	0.194	0.239
440	0.076	0.137	0.185	0.229
460	0.078	0.146	0.199	0.246
480	0.094	0.186	0.259	0.328
500	0.114	0.237	0.339	0.448
520	0.141	0.303	0.445	0.630
540	0.145	0.316	0.470	0.677
560	0.169	0.373	0.570	0.884
580	0.102	0.225	0.323	0.438
600	0.012	0.031	0.040	0.043
620	0.002	0.005	0.006	0.007
640	0.002	0.003	0.005	0.005
660	0.000	0.001	0.001	0.001
680	0.001	0.001	0.002	0.002
700	0.000	0.001	0.001	0.001
a_p	0.31	0.59	0.79	

Target #4 (Magenta)

nm	Dt 30	Dt 50	Dt 70	Ds
400	0.092	0.148	0.173	0.279
420	0.098	0.167	0.194	0.319
440	0.096	0.162	0.189	0.312
460	0.104	0.178	0.212	0.352
480	0.135	0.241	0.291	0.498
500	0.171	0.315	0.389	0.699
520	0.206	0.399	0.519	0.978
540	0.213	0.417	0.553	1.058
560	0.239	0.476	0.664	1.317
580	0.162	0.311	0.377	0.692
600	0.028	0.043	0.044	0.080
620	0.012	0.013	0.007	0.021
640	0.011	0.010	0.001	0.011
660	0.011	0.006	0.001	0.009
680	0.011	0.010	0.001	0.011
700	0.010	0.004	0.001	0.003
a_p	0.33	0.57	0.69	

Target #5 (Cyan)

nm	Dt 30	Dt 50	Dt 70	Ds
400	0.093	0.211	0.259	0.376
420	0.067	0.150	0.178	0.245
440	0.047	0.100	0.118	0.156
460	0.031	0.063	0.073	0.089
480	0.027	0.048	0.058	0.067
500	0.031	0.055	0.067	0.084
520	0.048	0.094	0.121	0.162
540	0.095	0.198	0.262	0.385
560	0.165	0.360	0.502	0.852
580	0.200	0.445	0.640	1.202
600	0.203	0.461	0.661	1.277
620	0.201	0.452	0.648	1.231
640	0.175	0.389	0.546	0.949
660	0.152	0.331	0.459	0.730
680	0.159	0.349	0.482	0.772
700	0.159	0.353	0.494	0.812
a_p	0.29	0.57	0.72	

Target #6 (Cyan)

nm	Dt 30	Dt 50	Dt 70	Ds
400	0.118	0.219	0.273	0.420
420	0.080	0.149	0.180	0.270
440	0.049	0.096	0.116	0.169
460	0.027	0.059	0.068	0.097
480	0.018	0.042	0.050	0.066
500	0.018	0.043	0.055	0.073
520	0.037	0.081	0.107	0.149
540	0.090	0.187	0.256	0.385
560	0.168	0.351	0.503	0.874
580	0.205	0.432	0.631	1.238
600	0.212	0.444	0.651	1.313
620	0.208	0.436	0.637	1.266
640	0.176	0.374	0.533	0.966
660	0.148	0.315	0.441	0.746
680	0.156	0.329	0.468	0.791
700	0.157	0.337	0.481	0.831
a_p	0.30	0.55	0.71	

Target	RMS Density Error
1 - Yellow	0.0123
2 - Yellow	0.0204
3 - Magenta	0.0091
4 - Magenta	0.0086
5 - Cyan	0.0078
6 - Cyan	0.0057
RMS Average:	0.0117

TABLE 2.

RMS Density Errors.

Error of the Spectral Predictions- The spectral densities of the solid patches and the dot areas of the tint blocks were used to predict the spectral densities of the tint blocks by applying the Yule-Neilsen model [in Equation (1)] at each of the wavelengths 400 [20] 700 nm. These predicted densities were compared to the densities actually observed, and the RMS Density Error for each target was computed. See Table 2.

The predicted densities were used to compute predictions of uniform color coordinates of the tint blocks. These predictions will be discussed below.

	TRISTIMULUS VALUES		
Target	X	Y	Z
1 - Yellow	81.93	91.27	8.63
2 - Yellow	82.39	91.62	8.70
3 - Magenta	62.82	41.80	44.67
4 - Magenta	54.59	31.06	34.57
5 - Cyan	19.44	29.98	62.96
6 - Cyan	18.86	30.04	61.93

These tristimulus values may be divided by 100 to yield reflectances on which the Yule-Neilsen model [as given in Equation (2)] may be applied to obtain wide-band predictions of the tristimulus values of the tints.

TABLE 3.

Tristimulus Coordinates of the Solids.

Wideband Predictions- The spectral densities of the solids were converted into wideband reflectances - the CIE Tristimulus Values X, Y, and Z. (Actually, the tristimulus values are reflectances multiplied by 100.) The tristimulus values of the solid patches are listed in Table 3. The standard 1931 color matching functions and standard graphic arts illuminant D-50 (5003 degrees Kelvin isotemperature daylight) were used to compute the tristimulus values.

These tristimulus values were used to compute the tristimulus values of the tint blocks, using the Yule-Neilsen model given in Equation (2). These were transformed into uniform color coordinates for comparison to the observed color.

CIELUV Color Coordinates- The CIE L^*, u^*, v^* (CIELUV) color coordinates of all patches were computed. These served as a standard against which the predictions may be judged. The two theories (spectral and wideband) were used to predict the CIELUV coordinates of the tint blocks. (For the case of the spectral theory, this was accomplished by first converting the spectral densities into reflectances, summing to obtain the tristimulus values, and converting the tristimulus values into the CIELUV coordinates. The wideband predictions were made in the form of tristimulus values, which were then transformed into the CIELUV coordinates.) These coordinates are listed in Table 4.

In Table 4, each patch is identified by the actual dot area as measured - rather than the "nominal" values as were used in Table 1. The "OB" legend refers to the color coordinates of the tint block as observed, and "SP" and "WB" are the predictions of the spectral and wideband theories, respectively. ΔE^* is the total color difference between a standard and a prediction; total color difference values were computed to compare the predicted colors to the observed as a measure of the error of a prediction.

DISCUSSION

A quick glance at both Table 1 (RMS Density Error) and Table 4 (CIELUV Color Coordinates) indicates an excellent fit of the spectral Yule-Neilsen model to these data. The RMS density errors are only slightly larger than we would expect from measurement error alone, and the overall RMS density error shows no statistical significance at five percent risk. The color predictions based on the spectral theory closely match the observed color coordinates, with an average color difference of 1.67. This would be judged adequate for most applications.

The wideband theory, on the other hand, seems unable to predict the color coordinates with reasonable accuracy. It is not possible to provide an across-the-spectrum measure of error as was computed for the spectral theory, so our discussion here involves only color differences in CIELUV space. The typical

Target #1 (Yellow)

Patch	L*	u*	v*	Δ E*
31% OB	98.44	4.48	31.13	
SP	98.80	4.73	32.51	1.45
WB	98.93	8.08	19.00	12.67
59% OB	98.17	8.36	58.66	
SP	97.79	9.00	59.03	0.82
WB	93.80	39.78	38.80	37.45
76% OB	97.54	11.44	72.26	
SP	97.21	11.59	72.58	0.48
WB	97.37	14.62	66.80	6.32
Solid	96.52	14.91	86.18	

Target #2 (Yellow)

Patch	L*	u*	v*	Δ E*
38% OB	98.27	5.14	37.17	
SP	98.61	5.89	39.22	2.20
WB	98.74	9.65	27.07	11.07
59% OB	97.65	9.82	61.44	
SP	97.72	10.07	63.12	1.70
WB	97.87	13.84	55.18	7.44
76% OB	97.73	15.24	10.84	
SP	97.25	12.36	74.49	1.66
WB	97.34	15.24	70.42	5.67
Solid	96.67	15.36	86.19	

Target #3 (Magenta)

Patch	L*	u*	v*	Δ E*
31% OB	91.35	23.23	-6.25	
SP	91.30	21.96	-8.24	2.36
WB	91.59	23.49	-20.67	11.07
59% OB	82.84	46.95	-15.00	
SP	83.80	43.26	-14.38	3.86
WB	83.53	46.77	-23.45	14.44
69% OB	76.60	66.11	-20.99	
SP	76.83	66.15	-23.04	2.06
WB	77.45	65.44	-25.72	4.82
Solid	70.74	87.34	-28.37	

TABLE 4.

CIELUV Color Coordinates - Observed and Predicted

Table 4 (Continued)

Target #4 (Magenta)

Patch	L*	u*	v*	ΔE*
33% OB	87.48	31.23	-10.84	
SP	87.43	32.26	-11.93	1.50
WB	88.81	30.68	-21.67	10.94
57% OB	78.45	58.32	-20.16	
SP	78.44	58.60	-20.22	0.29
WB	80.03	56.27	-24.94	5.44
69% OB	74.18	74.74	-25.65	
SP	73.82	73.31	-24.26	2.02
WB	75.41	70.50	-26.77	4.54
Solid	62.56	113.66	-32.26	

Target #5 (Cyan)

Patch	L*	u*	v*	ΔE*
29% OB	88.84	-20.92	-15.82	
SP	88.94	-21.74	-16.66	1.18
WB	89.99	-19.96	-28.14	12.41
57% OB	78.13	-41.91	-31.36	
SP	78.23	-43.10	-33.99	2.89
WB	87.51	-77.68	-14.77	40.53
72% OB	71.94	-53.96	-42.84	
SP	72.13	-54.85	-44.29	1.70
WB	73.65	-52.58	-46.74	4.49
Solid	61.63	-73.57	-62.08	

Target #6 (Cyan)

Patch	L*	u*	v*	ΔE*
30% OB	88.96	-23.29	-15.70	
SP	88.84	-22.38	-16.41	1.16
WB	89.65	-21.50	-27.97	12.42
55% OB	78.99	-41.98	-30.18	
SP	79.06	-42.59	-31.70	1.64
WB	80.38	-40.90	-37.75	7.78
71% OB	72.52	-54.59	-42.30	
SP	72.75	-55.58	-41.99	1.07
WB	74.07	-53.62	-44.91	3.20
Soild	61.69	-76.09	-60.08	

color difference between observed and the wideband prediction would normally be judged inadequate.

It seems worthwhile to point out that the largest color difference for the spectral theory was only slightly larger than the smallest color difference for the wideband theory. This would tend to indicate that the spectral model, at its worst, is no worse than the wideband model, at its best.

The spectral Yule-Neilsen model, however, is not absolved beyond every speck. The two largest RMS density errors (from Table 2) were for the two yellow targets. While this certainly might be a coincidence (the probability is 20 percent), it might indicate a lack-of-fit which was otherwise "buried in the grass" of experimental error.

Recall that Yellow is the "cleanest" of the process colors; that is, is has the least absorbtion in the bands it is supposed to reflect. It was wondered if this low absorbtion in the red (600 - 700 nm) and green (500 - 600 nm) bands might be difficult to predict. Analysis of the spectral density differences (from which the RMS density errors were calculated) showed relatively small deviations in the red and green bands, with most of the error in the blue (400 -500 nm) band.

CONCLUSIONS

It seems fair to assume that the Inverse Schwartz Inequality was the undoing of the wideband model. Reflectances across wide bands were summed together before being raised to the u-th power. Therefore, one would expect this type of problem with Status "T" densitometer measurements, as well. Measurements of this type were not made here because they would not provide a uniform measure of the color error. Nonetheless, it is expected that they would be high.

The spectral Yule-Neilsen model provided not only a good fit to the CIELUV color coordinates, but also to the spectral density curves. The matching of the spectral density curves is a more rigorous measure of fit because it detects possible metameric effects. In both cases, the model provided an acceptable prediction.

The only possible exception seemed to be with the yellow. A more detailed study of yellow tints, with more points of the spectrum included, and with acutal press-printed dots, would be interesting.

For use in quality control, where densitometers are used almost to the exclusion of spectrophotometers, it may be possible to use narrow-band densitometer readings to determine the entire spectrum of a tint or solid. This "bootstrapping" operation would probably involve non-linear equations, the solutions of which involve iterative processes.

Works in Progress- Because the Yule-Neilsen model was able to accurately predict the color of a monochrome halftone tint, it is hoped that a multicolor generalization will be able to predict the color of a multicolor overprint. An equation was derived (similar to the Neugebauer equations, but with the n value), and is in the process of being experimentally verified. Because of the effects of trapping, overlay proofing films may not be used, so actual press-printed dots will be analyzed.

In addition, a spectral version of the Tollenaar-Ernst model has been derived for the prediction of color in continuous tone.[5]

ACKNOWLEDGMENTS

The author would like to extend his sincere thanks to Dr. Julius Silver of RIT's School of Printing, Mr. Philip Tobias of Tobias Associates, Mr. George Leyda of 3-M, Mr. Irving Pobboravsky of the RIT Research Corporation, Mr. John Pagluica of Ridgewood Public Schools, and the author's other friends and family for their assistance on this project.

AUTHORITIES CITED

[1] Yule, J. A. C., and W. J. Neilsen, The Penetration of Light into Paper and its Effect on Halftone Reproduction. *1951 TAGA Proceedings,* p. 65 - 76.

[2] Viggiano, J. A. S., The GRL Dot Gain Model. *1983 TAGA Proceedings,* p. 423 - 439.

[3] Mauer, R. E., Color Measurements for the Graphic Arts. *1979 TAGA Proceedings,* p. 210.

[4] Pobboravsky, I., Methods of Computing Ink Amounts to Produce a Scale of Neutrals for Photomechanical Reproduction. *1966 TAGA Proceedings,* p. 13.

[5] Viggiano, J. A. S., *Models for the Prediction of Color in Graphic Reproduction Technology.* RIT Master's Thesis Proposal, 1985.

[6] Pearson, M., n Value for General Conditions. *1980 TAGA Proceedings,* p. 415 - 425.

[7] Viggiano, J. A. S., Color Matching Functions for Observers of Arbitrarily Sized Targets. *1984 TAGA Proceedings,* p. 61.

[8] Preucil, F., Color Diagrams. *1960 TAGA Proceedings,* p. 225 - 226.

[9] Wyszecki, G., and W. S. Stiles, *Color Science, 2nd Edition.* New York: John Wiley & Sons, 1982. p. 168.